MOLECULAR AND CELLULAR BIOLOGY, Dec. 1995, p. 6961–6970 Vol. 15, No. 12
0270-7306/95/$04.00+0

An Immunological Renal Disease in Transgenic Mice That Overexpress *Fli-1*, a Member of the *ets* Family of Transcription Factor Genes

LIQUN ZHANG,[1,2] ALLISON EDDY,[3] YEN-TUNG TENG,[1,2] MARVIN FRITZLER,[4] MICHAEL KLUPPEL,[1,5] FABRICE MELET,[1] AND ALAN BERNSTEIN[1,2,5]*

Program in Molecular Biology and Cancer, Samuel Lunenfeld Research Institute, Mount Sinai Hospital,[1] Institute of Medical Science[2] and Department of Molecular & Medical Genetics,[5] University of Toronto, and Department of Nephrology, Hospital for Sick Children,[3] Toronto, Ontario, and Department of Pathology, University of Alberta, Calgary, Alberta,[4] Canada

Received 21 June 1995/Returned for modification 29 July 1995/Accepted 10 August 1995

The proto-oncogene *Fli-1* is a member of the *ets* family of transcription factor genes. Its high expression in the thymus and spleen and the presence of DNA binding sites for *Fli-1* in a number of lymphoid cell-specific genes suggest that Fli-1 is involved in the regulation of lymphopoiesis. Activation of the *Fli-1* gene by either chromosomal translocation or viral insertion leads to Ewing's sarcoma in humans and erythroleukemia in mice, respectively. Thus, Fli-1 is normally involved in pathways involved in the regulation of cell growth and differentiation. We have generated *H-2K^k–Fli-1* transgenic mice that overexpress Fli-1 in various mouse tissues, with the highest levels of Fli-1 protein in the thymus and spleen. These *Fli-1* transgenic mice developed a high incidence of a progressive immunological renal disease and ultimately died of renal failure caused by tubulointerstitial nephritis and immune-complex glomerulonephritis. The incidences of renal disease correlated with the levels of Fli-1 protein in lymphoid tissues of transgenic lines. The hypergammaglobulinemia, splenomegaly, B-cell hyperplasia, accumulation of abnormal CD3$^+$ B220$^+$ T lymphoid cells and CD5$^+$ B220$^+$ B cells in peripheral lymphoid tissues, and detection of various autoantibodies in the sera of diseased *Fli-1* transgenic mice suggested the involvement of an immune dysfunction in the pathogenesis of the renal disease. In addition, splenic B cells from transgenic mice exhibited increased proliferation and prolonged survival in vitro in response to mitogens. Taken together, these data suggest that overexpression or ectopic expression of Fli-1 perturbs normal lymphoid cell function and programmed cell death. Thus, *H-2K^k–Fli-1* transgenic mice may serve as a murine model for autoimmune disease in humans, such as systemic lupus erythematosus.

The members of the *ets* gene family encode a highly conserved group of sequence-specific DNA-binding proteins (20, 27). To date, more than 25 *ets* gene family members that share significant amino acid similarity with their founding member, the v-*ets-1* oncogene, have been described. This region of homology, the so-called ETS domain is responsible for the sequence-specific DNA-binding activities of these proteins. Ets family members bind to a purine-rich DNA sequence that includes an invariant GGA core sequence, flanked by 5 to 8 nucleotides (nt) of surrounding sequence that define the particular DNA-binding specificities of individual *ets* family members (20, 27). Various Ets proteins can function as transcription factors through their binding to specific DNA binding sites that are found in a wide variety of viral and cellular transcriptional regulatory regions (20, 33). In addition, *ets* genes are developmentally regulated and expressed in a variety of tissues, including cells of hematopoietic lineages (13, 19, 27). Many members of the *ets* gene family, including c-*ets-1* and -*2*, *Fli-1*, *erg*, *Spi-1*, and *tel*, possess oncogenic activity when activated as a result of chromosomal translocations or proviral insertions (3, 8, 12, 35). These observations implicate *ets* family members in important developmental processes and oncogenesis.

The mouse *Fli-1* (Friend leukemia integration site 1) gene was originally identified as the proto-oncogene insertionally activated in 75% of erythroleukemia cell clones induced by Friend murine leukemia virus (3). The human homolog of *Fli-1* is rearranged in Ewing's sarcoma and neuroepithelioma as a result of a reciprocal chromosomal t(11;22) translocation that fuses the DNA-binding ETS domain of Fli-1 to a novel N-terminal sequence of a gene called EWS derived from chromosome 22 (8). The EWS–Fli-1 fusion protein, a chimeric transcriptional factor, is strongly transforming for fibroblasts in vitro and the ETS domain of Fli-1 is required for its transforming activity (21). Thus, Fli-1 is involved in malignancies in both humans and mice.

We have previously shown that the Fli-1 protein has distinct but overlapping DNA-binding activities with other Ets proteins in vitro (33). For example, *Fli-1* and *Erg-2* have identical DNA-binding specificities and their DNA-binding ETS domains have 98% amino acid sequence identity (3). Consistent with this high degree of sequence identity and DNA-binding specificity, several cases of Ewing's sarcoma in which the EWS sequence is fused to the ETS domain of *Erg*, not *Fli-1*, have been described (35). The *Fli-1* gene is highly expressed in hematopoietic tissues and cells, including the thymus and spleen (3, 17). Like some other Ets proteins, Fli-1 is expressed at high levels in lymphoid tissues. For example, *Fli-1*, *Ets-1*, *Ets-2*, *Elf-1*, and *GABP*α are all expressed in T cells (17, 19), while *Fli-1*, *Ets-1*, *Spi-1*, and *Erg-3* are expressed in B cells (13, 25). Furthermore, many lymphoid cell-specific genes, including the genes that encode the T-cell receptor β chain, granulocyte-macrophage colony-stimulating factor, interleukin-3 (19), the human immunodeficiency virus type 2 long terminal repeat, terminal de-

* Corresponding author. Mailing address: Program in Molecular Biology and Cancer, Samuel Lunenfeld Research Institute, Mount Sinai Hospital, 600 University Ave., Toronto, Ontario, Canada M5G 1X5. Phone: (416) 586-8273. Fax: (416) 586-8844.

oxytidyl transferase, immunoglobulin heavy chain, and λ5 light chain (13), and the *lck* promoter (22), all contain a consensus binding site (-[C/A]GGAA[C/G]-) in their regulatory elements for Fli-1 and possibly other Ets proteins. Taken together, these observations suggest that Fli-1 and perhaps other Ets proteins play critical roles in lymphoid differentiation and function.

In order to study the biological functions of Fli-1 in vivo, we have generated transgenic mice that overexpress Fli-1. These transgenic mice develop, at high incidence, an immunological renal disease that is associated with immune-complex glomerulonephritis, accumulation of autoantibodies and autoreactive B or T cells, splenomegaly, B-cell hyperplasia, and hypergammaglobulinemia. In addition, B cells from *Fli-1* transgenic mice are hyperresponsive to mitogens and exhibit significant reduction in activation-induced cell death and prolonged survival in culture compared with B cells from nontransgenic control mice in vitro. These data suggest that Fli-1 is an important regulator of lymphoid cell function and programmed cell death.

MATERIALS AND METHODS

Construction of the *H-2K^k–Fli-1* transgene. A 1.73-kb *Eco*RI DNA fragment encompassing the complete coding region of Fli-1 was isolated from the *Fli-1* cDNA clone BB4 (2). The *H-2K^k* class I gene promoter was cloned as a 1.9-kb *Hin*dIII-*Eco*RI fragment from pUCH2K^{kP} (a gift from Martin Breitman). An 0.24-kb *Eco*RI-*Bam*HI DNA fragment that contains the simian virus 40 polyadenylation site was derived from the vector pECE (9). These DNA fragments were subcloned into the plasmid pKS$^+$ between the *Hin*dIII and *Bam*HI sites to yield the plasmid pKS$^+$/H2K^k-Fli-1 (Fig. 1A).

Generation and maintenance of transgenic mice. All animals were maintained under specific pathogen-free conditions in micro-isolator cages and were handled in accordance with animal care guidelines. We produced transgenic mice in the CD-1 outbred strain by standard oocyte injection methods (1). The *H-2K^k–Fli-1* transgene used for microinjection was approximately 4 kb in length and isolated by digesting the plasmid pKS$^+$/H2K^k-Fli-1 with *Xho*I and *Spe*I (Fig. 1A). Of 200 eggs injected with this *Xho*I-*Spe*I DNA fragment, 30 pups survived to adulthood, and of these 30 pups, 3 transgenic founders were identified by genomic Southern blot analysis. Transgenic mice were identified by probing Southern blots of *Bam*HI-digested tail DNA (5 μg) with a ^{32}P-labelled random-primed 1.73-kb *Eco*RI fragment isolated from the *Fli-1* cDNA clone BB4. The transgene positive founders were bred with healthy CD-1 mice to establish three independent transgenic lines (B6, B7, and B8).

RNase protection analysis of transgene expression. RNA samples were prepared from adult tissues by Polytron homogenization in 4 M guanidium isothiocyanate, followed by phenol-chloroform extraction and isopropanol precipitation (5). T7 antisense riboprobe (200 nt) was synthesized and hybridized to total RNA samples, essentially as described by the supplier (Promega). The HB probe protects a 175-nt fragment from the transgene transcript and a 150-nt fragment of the endogenous *Fli-1* transcript. To achieve comparable signals, we synthesized a β-actin probe (57 nt) at 1/10 the specific activity of the HB probe. After hybridization at 50°C overnight, samples were digested with 40 μg of RNase A per ml and 2 μg of RNase T_1 (Ambion) per ml for 1 h at 37°C. Protected fragments were separated on 6% polyacrylamide–8 M urea sequencing gels, which were then dried and exposed for autoradiography with Kodak XAR-5 film and an intensifying screen. An optical dosimeter was used to measure the intensity of each band.

In situ RNA hybridization. In situ RNA hybridization was performed on 8-μm-thick cryostat sections, as described previously (23). Adjacent sections were probed with *Fli-1* antisense and sense RNA probes. The *Fli-1* antisense probe, spanning nt 1396 to 1729 of the murine *Fli-1* gene, was generated by T7 RNA polymerase from the *Eco*RV-linearized DNA template of p-GEM7-Fli-1 (BB4) and the *Fli-1* sense probe, spanning nt 1 to 453 of the murine *Fli-1* gene, was generated by SP6 RNA polymerase (Boehringer Mannheim) from *Bam*HI-linearized DNA template of BB4. Following hybridization, the slides were washed for 30 min; this wash was followed by two stringent washes of 20 min each at 60°C in 0.1× standard saline citrate (15 mM NaCl, 1.5 mM sodium citrate; pH 7). The slides were dipped in Kodak NTB-2 emulsion, exposed for 4 to 15 days, developed, and stained with toluidine blue.

Western blot (immunoblot) analysis. Different tissue extracts were obtained by lysing mouse tissues in radioimmunoprecipitation assay buffer (33) at 4°C by Polytron homogenization. Equivalent amounts of tissue extracts were loaded into all lanes of a 10% sodium dodecyl sulfate protein gel on the basis of measurement of bicinchoninic acid protein assays (Pierce). After gel electrophoresis, the separated proteins were transferred onto nitrocellulose membranes (Bio-Rad Laboratories) with a semidry transfer apparatus. After treatment with a blocking solution (0.5% milk, 0.05% Tween 20, 1× Tris-buffered saline) overnight at 4°C, the filter was exposed to 5 μg of affinity-purified anti-Fli-1 antisera (33) for 2 h at room temperature, washed, and probed for 1 h with a 1:2,000 dilution of a goat anti-rabbit immunoglobulin G (IgG) conjugated to horseradish peroxidase (Bio-Rad). After a final wash, bands were revealed by enhanced chemiluminescence (ECL kit from Bio-Rad) and exposure to X-ray film. The anti-Fli-1 antiserum (R8 [33]) detects Fli-1 proteins of 51 and 48 kDa in various mouse tissues. The relative Fli-1 protein levels in each tissue were determined by the measurement of Fli-1 bands with an optical densitometer (WP700).

Histological analysis. Freshly dissected tissues were fixed in 10% formalin solution. Fixed specimens were embedded in paraffin, sectioned, and stained with hematoxylin and eosin stain. For immunohistochemistry, freshly dissected tissues were snap-frozen in isopentane precooled in liquid nitrogen and stored at −70°C. Five-micrometer-thick cryostat sections were stored at −20°C. The sections were fixed for 10 min in acetone at 4°C. Sections were washed in phosphate-buffered saline (PBS) and then incubated with the fluorescein isothiocyanate (FITC)-conjugated antibodies at a dilution of 1:50 for 30 min at room temperature in a wet chamber. The sections were then washed in PBS with 0.2% Triton X-100 for 5 min (each) three times. Sections were mounted and examined by fluorescence microscopy. The polyclonal antisera used were as follows: FITC-conjugated rat anti-mouse polyvalent immunoglobulins (IgM, IgG, and IgA) (Serotec), anti-C3 (Serotec), and anti-rat IgG (heavy plus light chains) (Cedarlane). The monoclonal antibodies used were as follows: anti-IgM (MCA 199; Serotec), anti-IgG (MCA 424; Serotec), and anti-IgA (MCA 471; Serotec).

Enzyme-linked immunosorbent assays. Polystyrene plates with 96 flat-bottom wells were coated first with 1 μg of antibodies against either murine IgG, IgA, or IgM in PBS for 1 h and then blocked with 3% bovine serum albumin in PBS for 30 min. After the wells were washed three times with PBS–0.05% Tween 20, the different dilutions of serum samples were added and incubated for 1 h in room temperature. After three further washes, a dilution of 1:10,000 with a horseradish peroxidase-conjugated polyclonal antibody against mouse IgG, IgA, and IgM (IgGAM) was added to the wells coated with IgG, and a dilution of 1:1,000 was added to the wells coated with either IgM or IgA. After incubation and washing, the measurement of peroxidase conjugates in the presence of substrates (Bio-Rad) was expressed as A_{575} (10^3). Standard deviations did not exceed 15% of the mean. Polyclonal antisera used were goat anti-mouse IgM (Sigma), goat anti-mouse IgG (Sigma), goat anti-mouse IgA (Sigma), and horseradish peroxidase-conjugated goat anti-mouse IgGAM (Sigma).

Indirect immunofluorescence. Autoantibodies directed against cellular antigens were first evaluated on the basis of indirect immunofluorescence microscopy by using a commercial ANA kit (ANA2000). Fluorescein-conjugated rabbit anti-mouse immunoglobulin secondary antibody was used at dilutions determined after appropriate titration against negative- and positive-control MRL/*lpr* sera.

Anti-DNA antibodies. Autoantibodies directed against double-stranded DNA were determined by indirect immunofluorescence with a *Crithidia lucilliae* substrate as previously described (11). Control sera from MRL/*lpr* mice with anti-double-stranded DNA antibodies were included with every test.

Flow cytometry. Cell preparations for flow cytometry were obtained by crushing freshly dissected tissues between flat forceps in 1× PBS. Cells were concentrated by centrifugation and resuspended in 1× PBS. A total of 10^6 cells were incubated with primary FITC- or phycoerythrin-conjugated antibodies in 1× PBS with 1% fetal calf serum for 30 min at 4°C. Cells were washed twice in PBS, resuspended in 400 μl of 1% formaldehyde in PBS, and analyzed on a flow cytometer (Epic C). Monoclonal antibodies used for analysis included phycoerythrin-conjugated anti-mouse B220 (RA3-6B2; Pharmingen), FITC-conjugated anti-mouse CD3 (145-2C11; Pharmingen), and FITC-conjugated anti-mouse CD5 (53-7.8; Pharmingen).

In vitro B-cell functional assays. Single-cell suspensions were prepared from the spleens of transgenic and control mice and B cells were enriched by using anti-Thy-1 antibody (G7; Pharmingen) (3 to 5 μg/ml/5 × 10^6 cells) and rabbit complement (1:12 dilution), as described in *Current Protocols in Immunology* (13a). The resulting B-cell population was >90% B220$^+$ and <5% Thy-1$^+$ by flow cytometry. B cells were plated at 10^5 cells per well and cultured in RPMI 1640 complete medium with 5% (vol/vol) newborn calf serum. Wells were harvested on day 1, 2, 3, 4, or 5, and viable cells were counted by using trypan blue. Cells were incubated in triplicate with lipopolysaccharide (LPS) (Sigma) or anti-IgM (μ chain specific; Sigma) for 2 to 3 days. The concentrations of LPS and anti-IgM are indicated in the figure legends. Then, 1 μCi (37 kBq) of [^{3}H]thymidine (Amersham) was added per well, and the culture was incubated for an additional 16 h before harvesting and determination of [^{3}H]thymidine incorporation. For propidium iodide staining, B cells were cultured with the same medium at 10^6 cells per ml in 5-ml flasks. At different time points, 0.5 × 10^6 cells were washed in PBS and resuspended in 0.2 ml of PBS with 50 μg of propidium iodide (Sigma) per ml. Samples were kept at 4°C in the dark before flow cytometric analysis with a FACScan flow cytometer.

Statistics. Student's *t* test was used to determine the statistical significance of differences between groups. A P value of <0.05 was considered significant.

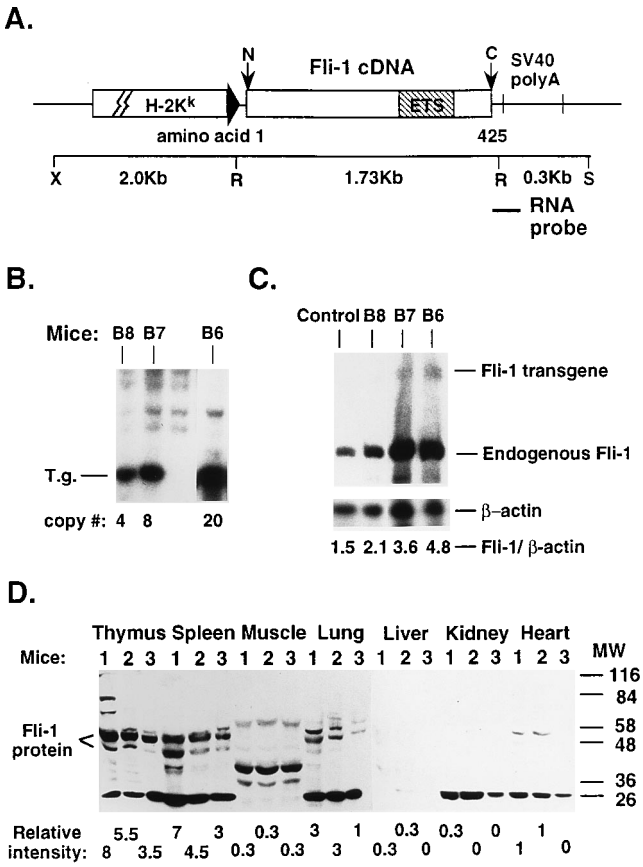

FIG. 1. (A) The *H-2K^k–Fli-1* transgene construct used to generate *Fli-1* transgenic mice. The 1.73-kb fragment of *Fli-1* cDNA (15) was fused to the *H-2K^k* class I gene promoter (19) at its 5′ end and the simian virus 40 poly(A) (SV40 polyA) sequence at its 3′ end. Abbreviations: X, *Xho*I; R, *Eco*RI; S, *Spe*I; N, N-terminal amino acid; C, C-terminal amino acid. (B) Genomic Southern blot analysis. Samples (5 μg) of DNA from three transgenic founders (B6, B7, and B8) and control mice were digested with *Bam*HI to generate a 1.45-kb *Fli-1* cDNA fragment from the *Fli-1* transgenic mice. The relative transgene copy numbers of each transgenic line were indicated below the gel. T.g., transgene. (C) *Fli-1* transgene RNA expression in spleens determined by an RNase protection assay. The 125-nt riboprobe (panel A) was used to protect a 115-nt transcript of the *Fli-1* transgene and a 95-nt transcript of the endogenous *Fli-1* gene. The level of β-actin transcripts in each RNA sample was measured as an internal control. The ratios of the band intensities corresponding to endogenous *Fli-1* transcripts and those of β-actin transcripts within the same RNA sample were calculated as the relative endogenous *Fli-1* mRNA levels in the spleens and indicated below the gel. (D) Western blot analysis of Fli-1 protein expression. Mouse 1, a 6-week-old B6 transgenic mouse; mouse 2, a 6-week-old B7 transgenic mouse; and mouse 3, a 6-week-old wild-type littermate. Equivalent amounts of tissue extracts isolated from three mice were loaded into each lane on the basis of measurement of bicinchoninic acid protein assays (Pierce). The anti-Fli-1 antiserum (R8 [33]) detects Fli-1 proteins of 51 and 48 kDa. The relative intensities of the Fli-1 protein bands were quantitated by densitometry (WP700).

RESULTS

***H-2K^k–Fli-1* transgenic mice and *Fli-1* gene expression.** A 1.73-kb complementary DNA encoding the mouse Fli-1 protein was fused to the promoter region of the mouse *H-2K^k* gene (16) and injected into zygotes of CD-1 mice (Fig. 1A). The *H-2K^k* promoter is known to direct heterologous transgene expression in a wide variety of mouse tissues (6). Southern blot analysis of genomic DNA digested with *Bam*HI and hybridized with a *Fli-1* cDNA probe was used to identify three founder lines of *H-2K^k–Fli-1* transgenic mice (Fig. 1B). Founders B6, B7, and B8 carried 20, 8, and 4 transgene copies, respectively, and were bred to establish the B6, B7, and B8 transgenic lines described here. *H-2K^k–Fli-1* transgene expression was confirmed by RNase protection assays and by Western blot analysis of the total cellular proteins of different tissues from three transgenic lines. Using a 200-nt RNA probe which distinguishes transcripts encoded by the transgene and the endogenous *Fli-1* gene, we detected *Fli-1* transgene expression in all tissues tested, including brain, heart, kidney, liver, lung, muscle, spleen, and thymus tissues (data not shown). In addition, the levels of endogenous *Fli-1* transcripts were also elevated in the lymphoid tissues of *Fli-1* transgenic mice (Fig. 1C). This relative increase in endogenous *Fli-1* expression appears to reflect the levels of transgene expression, suggesting that *Fli-1* might act to positively regulate its own expression. The steady-state Fli-1 protein levels in B6 and B7 lines were also approximately two- to threefold higher than that of the control, as determined by Western blotting (Fig. 1D).

Pathology of a chronic renal disease in *Fli-1* transgenic mice. Transgenic pups were visually indistinguishable from control littermates. However, within 6 to 18 months, a chronic renal disease developed in these mice, although the timing and severity varied between individual mice, even within a given transgenic line. Gross examination of *Fli-1* transgenic mice revealed enlarged kidneys with cortical scars (early stage), and in the late stage, the kidneys were yellow and shrunken (Fig. 2a). Examination by light microscopy revealed that *Fli-1* transgenic mice developed a renal disease characterized by progressive tubulointerstitial nephritis and glomerulonephritis. Before overt renal disease was evident, histological analysis revealed the presence of a few small foci of interstitial mononuclear cells that were less frequently observed in the kidneys of control littermates (data not shown). By 3 to 6 months of age, a high proportion of *Fli-1* transgenic mice had developed early-stage tubulointerstitial nephritis characterized by increased interstitial infiltration of mononuclear cells mainly around blood vessels and <10% tubule atrophy or dilation (data not shown). Small protein casts were also observed within the lumina of dilated tubules. At this stage, glomerular mesangial cell proliferation was present but no deposits were observed within the glomeruli by light microscopy. Between 6 and 18 months of age, late-stage renal disease, associated with significant progression of tubulointerstitial nephritis, massive mononuclear cell infiltration, >50% tubule atrophy, and dilated tubules filled with large protein casts, developed in these mice (Fig. 2c). In addition, the glomeruli of late-stage diseased transgenic mice either became fibrotic or were enlarged and filled with massive homogeneous protein deposits (Fig. 2c), as confirmed by positive staining with periodic acid-Schiff stain and negative staining with Congo red (data not shown). Massive electron-dense deposits could also be observed by electron microscopy within the mesangial regions of the enlarged glomeruli.

These mice also developed proteinuria, a sign of glomerular dysfunction. Proteinuria was first detected at 4 to 6 months of age in the early stage and increased gradually (data not shown). Eventually, all diseased mice died of renal failure between the ages of 6 to 18 months. For example, one mouse died at 6 months with a high serum creatinine level (110 μmol/liter) and significant proteinuria (12,600 μg/liter), indicating extensive loss of renal glomerular function. In contrast, normal littermates at the same age had low serum creatinine levels (40 μmol/liter) and low proteinuria (500 μg/liter).

Immunopathogenesis of the renal disease in *Fli-1* transgenic mice. The morphologic features observed by light and electron microscopy suggested an immunological basis as the underlying pathogenetic mechanism involved in the chronic glomerulonephritis that developed in *Fli-1* transgenic mice. By

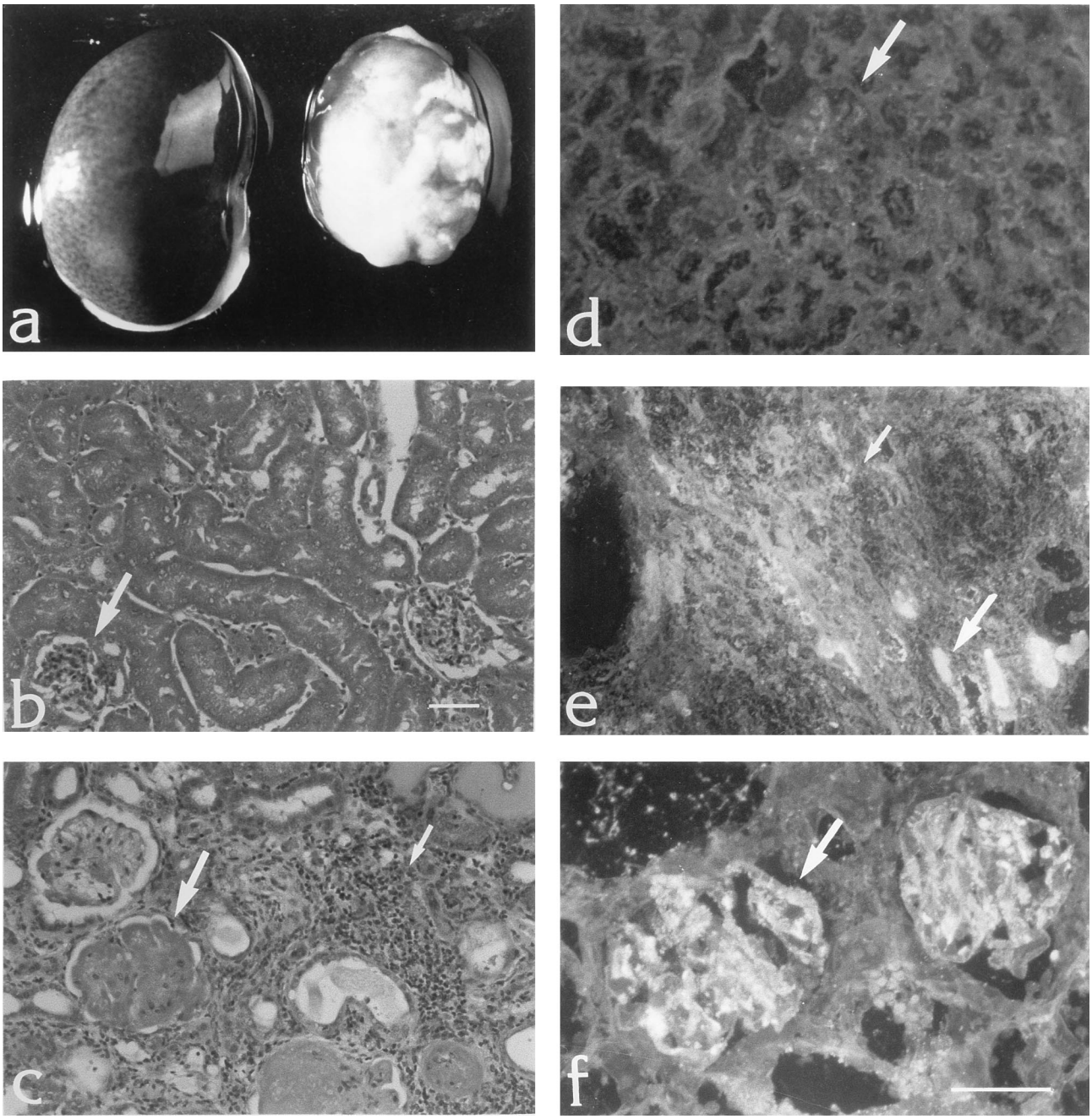

FIG. 2. Histological analysis of *Fli-1* transgenic mice. (a) Photograph of a normal kidney (left) and a late-stage diseased kidney (right). (b) Light photomicrograph of a normal kidney at 12 months of age (hematoxylin and eosin stain). The arrow points to a normal glomerulus. Magnification, ×250. Bar, 0.1 mm. (c) Light photomicrograph of the kidney of a *Fli-1* transgenic mouse (B8) at 18 months of age, illustrating advanced tubulointerstitial and glomerular disease. The tubulointerstitial nephritis is characterized by regions of tubular ectasia and atrophy and interstitial fibrosis, in addition to the persistence of a significant infiltrate of mononuclear cells (small arrow). The glomeruli are enlarged and either have a lobular configuration characteristic of membranoproliferative glomerulonephritis (large arrow) or are becoming sclerotic. The glomeruli are filled with massive deposits of pink-staining material which also reacted with periodic acid-Schiff stain (hematoxylin and eosin stain). Magnification, ×250. (d) A normal kidney section stained with an FITC-conjugated goat anti-mouse IgAGM shows minimal staining of the glomerulus (arrow). (e) Kidney section of a B6 transgenic mouse (8 months of age) stained with an FITC-conjugated anti-mouse IgGAM antibody illustrates positive staining of infiltrating B lymphocytes (small arrow) and tubular casts (large arrow). Magnification, ×400. (f) The kidney of a *Fli-1* transgenic mouse (B7) at 6 months of age stained with an FITC-conjugated anti-mouse IgGAM antibody, illustrating positive interstitial cells, tubular casts, and granular deposits within the glomerulus (arrow). Magnification, ×400. Bar, 0.1 mm.

immunofluorescence microscopy, a large proportion of the infiltrating interstitial mononuclear cells were surface IgG, IgA, or IgM positive (Fig. 3b), suggesting that they were immunoglobulin-secreting B lymphocytes. The protein casts in the dilated tubule lumen also reacted with antiimmunoglobulin antibodies (IgG > IgA > IgM) (Fig. 3b). When significant proteinuria developed, polyclonal IgG and IgA (but not IgM) were detected in the urine and gradually increased, as determined by immunoelectrophoresis (data not shown). Together, these data suggest that serum immunoglobulin leaked out into the urine as a result of glomerular injury.

The deposits in the glomeruli observed by immunofluores-

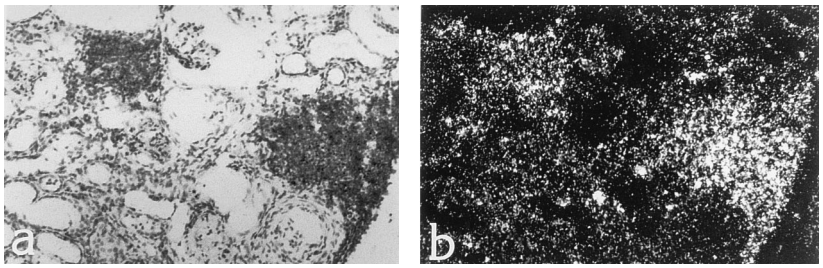

FIG. 3. RNA in situ hybridization analysis of *Fli-1* expression in diseased kidneys. The section was hybridized with a *Fli-1*-specific probe. Bright-field (a) and dark-field (b) photomicrographs of adult kidney sections from a B6 transgenic mouse.

cence microscopy in the late stage of renal disease reacted in an irregular granular pattern with FITC-conjugated antibodies against IgG, IgA, and IgM (IgM > IgG > IgA) (Fig. 2f). In addition, granular deposits of complement C3 were also detected in these enlarged glomeruli (data not shown). The appearance of intraglomerular electron-dense deposits and their reactivities with antibodies against immunoglobulins and complement C3 suggest that these deposits are immune complexes, although the nature of the target antigen is unknown. Of note, no immune complexes were detected in the interstitium, along tubular basement membranes, or within the walls of extraglomerular renal vessels.

High incidence of immune-complex renal disease in *Fli-1* transgenic mice. Table 1 summarizes the phenotypes of the early and late stages of the renal disease that developed in *Fli-1* transgenic mice. The mice with early-stage renal disease had early or minor tubulointerstitial nephritis, and the mice with late-stage renal disease had tubulointerstitial nephritis of variable severity and glomerulonephritis. To date, a total of 45 B6 mice, 25 B8 mice, 13 B7 mice, and 62 control littermates have been analyzed. In summary, both the B7 and B6 transgenic lines developed both early-stage (100%) and late-stage (67 to 87%) renal disease at high frequency. The low incidence of late renal disease in the B8 transgenic line was similar to that of control mice (8%), possibly reflecting the low transgene expression in this transgenic line.

***Fli-1* expression in kidneys.** To determine whether the renal phenotype of *Fli-1* transgenic mice was related to *Fli-1* transgene expression in the kidney, we analyzed *Fli-1* expression in nondiseased and diseased kidneys. Prior to the onset of nephritis, the kidneys of transgenic mice expressed the same levels of *Fli-1* transcripts as those of control mice and only low levels of Fli-1 protein were detected in the kidneys of B6 and B7 mice (data not shown). During progression of the renal disease, the levels of Fli-1 protein gradually increased, as detected by Western blotting (data not shown). To determine whether this increase in *Fli-1* expression in the kidneys resulted from the massive accumulation of infiltrating lymphocytes in these mice, we carried out RNA in situ hybridization analysis. As shown in Fig. 3, high levels of *Fli-1* transcripts were detected only in the infiltrating mononuclear cells in the kidneys of diseased transgenic mice.

TABLE 1. Progression of the renal disease in *Fli-1* transgenic mice

Characteristic	Phenotype of diseased mice[a]	
	Early stage	Late stage
Tubulointerstitial lymphocytic infiltration	++	++++
Dilated tubules filled with protein casts stained for IgG, IgA, and IgM (IgG > IgA > IgM)	−/+	++++
Tubular atrophy	+	++++
Mesangial cell proliferation, mesangial electron-dense deposits	−/+	++++
Massive glomerular deposits stained for IgG, IgA, and IgM (IgM > IgG > IgA) and C3	−	++++
Proteinuria	−/+	++++
Renal failure and death	−	++++

[a] Summary of the early- and late-stage phenotypes of the diseased mice. The mice with early-stage renal disease had early tubulointerstitial nephritis, and the mice with late-stage renal disease had advanced tubulointerstitial nephritis and glomerulonephritis. Symbols: −, phenotype of healthy mice; −/+, small changes from healthy phenotype; +, mild changes in phenotype; ++, moderate changes in phenotype; ++++, drastic changes in phenotype.

Immune dysfunction in *Fli-1* transgenic mice. The histological and RNA in situ analysis described above suggests that the immune-complex-mediated renal disease was associated with massive interstitial infiltration by lymphoid cells expressing high levels of *Fli-1* transcripts. Because Fli-1 is normally expressed in lymphoid cells and the DNA binding sites for Fli-1 are present in many lymphoid cell-specific genes (13, 18, 19), we next investigated whether perturbations in the immune system might explain the renal disease in the *Fli-1* transgenic mice.

Analysis of infiltrating lymphocytes in diseased kidneys. Initially, we determined the surface phenotypes of the interstitial infiltrating lymphocytes in the kidneys of control and diseased mice. In the kidneys of diseased mice, between 34 and 42% of the interstitial infiltrating mononuclear cells were $CD4^+$ helper T lymphocytes, 7 to 8% were $CD8^+$ cytotoxic T cells, and approximately 40% were Ig^+ B lymphocytes and plasma cells. The accumulation of plasma cells in the diseased kidneys was also evidenced by light microscopy. Therefore, both T and B lymphoid cells were associated with the progression of renal disease. The accumulation of immunoglobulin-secreting B cells in the diseased kidneys of *Fli-1* transgenic mice might also play an important role in the immunopathogenic process of the immune-complex renal disease.

Splenomegaly, B-cell hyperplasia, and hypergammaglobulinemia. To investigate these immunological alterations further, we analyzed the peripheral lymphoid organs in *Fli-1* transgenic mice. None of the *Fli-1* transgenic mice developed lymphadenopathy. The total cell number of lymph nodes in diseased transgenic mice was twice those of healthy and control mice (Table 2). However, the spleens of all mice with early renal disease and of half of the mice with late renal disease were three to eight times larger than those of control littermates or healthy transgenic mice. Similarly, the total number of spleen cells from the diseased transgenic mice was significantly higher than those of control mice and healthy transgenic mice (Table 2). In addition, increases in the relative numbers of mature B cells ($B220^+$ Ig^+) within both lymph nodes and

TABLE 2. Total cell numbers and proportions of B cells in lymph nodes and spleens[a]

Mice	Lymph node		Spleen	
	Total no. of cells (10^6)	$B220^+$ Ig^+ cells (%)	Total no. of cells (10^6)	$B220^+$ Ig^+ cells (%)
Control	19 ± 11	6 ± 4	159 ± 78	36 ± 7
Healthy transgenic	27 ± 9	10 ± 5	242 ± 107	43 ± 11
Diseased transgenic	**43** ± 14	**43** ± 7	**627** ± 158	**61** ± 15

[a] Total cell numbers in the lymph nodes and spleens of *Fli-1* transgenic and control mice, as determined by trypan blue exclusion. The number of Ig^+ B cells was determined by using antibodies directed against murine B220 and immunoglobulin. Each value listed in the table is the average ± standard deviation of a number of mice ($n > 10$). The values in boldface type are those values that were significantly higher than those of control mice and healthy transgenic mice.

spleens of diseased transgenic mice were observed (Table 2), suggesting that B-cell hyperplasia or B-cell activation had occurred during the progression of immune-complex renal disease in the *Fli-1* transgenic mice. In addition to B-cell hyperplasia, B6 and B7 transgenic mice at 1 to 4 months of age had increased serum IgG, IgA, and IgM levels (data not shown). The same serum samples had increased levels of polyclonal IgG, IgA, IgM, and κ and λ light chains relative to those in control sera and had no monoclonal immunoglobulin peaks by immunoelectrophoresis (data not shown). Therefore, the polyclonal B-cell activation in *Fli-1* transgenic mice was evidenced by hypergammaglobulinemia detected in the early stage of renal disease.

Accumulation of autoreactive lymphocytes and autoantibodies in vivo. Immune-complex glomerulonephritis was suggestive of an etiology of immune dysfunction (10). Consistent with this possibility were striking increases in both abnormal T ($CD3^+$ $B220^+$) and B lymphocytes ($CD5^+$ $B220^+$) in the lymph nodes, spleens, and kidneys of the late-stage diseased transgenic mice (Fig. 4). The double-positive $CD3^+$ $B220^+$ T cells were also Thy-1^+ $CD4^-$ $CD8^-$ (data not shown) and the double-positive $CD5^+$ $B220^+$ B cells were also IgM^+ (data not shown). Normally, CD3 is expressed only on T cells and B220 is expressed only on B cells. Double-positive $CD3^+$ $B220^+$ T cells also accumulate to high levels in the enlarged lymph nodes of autoimmune *lpr/lpr* mice (7, 34). Only small numbers of double-positive $CD5^+$ $B220^+$ B cells exist in normal peripheral lymphoid tissues. However, these $CD5^+$ B cells accumulate in autoimmune NZB/NZW mice (14) and are likely responsible for the autoimmune hemolytic anemia in these mice as a result of their synthesis of IgM autoantibodies (15). Therefore, the emergence of these potentially autoreactive T and B lymphoid cell populations in *Fli-1* transgenic mice in the late stage of renal disease is strikingly similar to the cellular changes observed in other murine models of autoimmune disease. Additionally, antinucleus autoantibodies were detected in all transgenic mice but in only one of seven control mice (Table 3). By contrast, only diseased transgenic mice (50%)

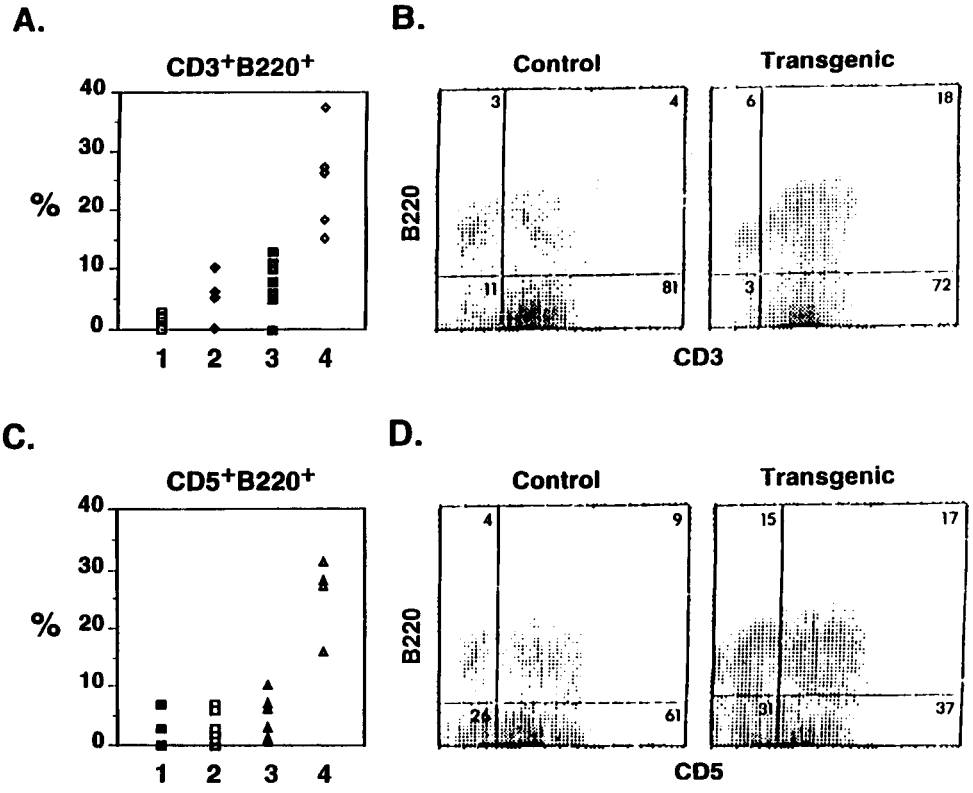

FIG. 4. Fluorescence-activated cell sorter analysis of abnormal lymphocytes from control and *Fli-1* transgenic mice. (A and C) Graphic summaries of flow cytometry data. Cells prepared from the lymph nodes of control mice and *Fli-1* transgenic mice with either early- or late-stage renal disease were analyzed with antibodies directed against murine B220, CD3, and CD5. Each column shows the relative values for the percentages of $CD3^+$ $B220^+$ and $CD5^+$ $B220^+$ cells from each mouse group. Group 1, control mice; group 2, healthy transgenic mice; group 3, early-stage diseased transgenic mice; group 4, late-stage diseased transgenic mice. (B and D) Two-color immunofluorescence contour plots of B220 and CD3 or B220 and CD5 expression on lymph node cells from a 6-month-old diseased transgenic mouse and a control littermate. Fluorescence intensity is shown on a log-log scatter plot. The percentage of cells within each quadrant is indicated. Similar data were obtained with cells derived from the spleens of these mice (data not shown).

TABLE 3. Autoantibodies in *H-2K^k–Fli-1* transgenic mice[a]

Mice	No. of mice with antibody/total no. of mice tested	
	Anti-DNA	Antinucleus
Control	0/7	1/7
Healthy transgenic	0/4	4/4
Diseased transgenic	4/8	7/8

[a] Antinucleus and anti-DNA antibodies in *Fli-1* transgenic and control mice. Results are expressed as the number of mice with positive samples compared with the total number of animals tested.

showed the presence of anti-DNA autoantibodies. In addition, three of eight diseased transgenic mice displayed autoantibody staining of nuclei containing antibodies against small nuclear ribonucleoprotein antigens present in nuclei (data not shown). In humans, the latter activity is uniquely, although not uniformly, associated with the autoimmune disease systemic lupus erythematosus (29).

Hyperresponsiveness and prolonged survival of transgenic B cells in vitro. Consistent with the *Fli-1* expression pattern in the spleens of mice from the B6 line, the levels of Fli-1 protein in purified B cells from B6 transgenic mice were three times more abundant than in B cells from control littermates (data not shown). Because B-cell hyperplasia in other autoimmune mouse models (Table 4) can result from alterations in lymphocyte function and/or cell survival, it was possible that *Fli-1* overexpression interferes with proliferation and/or cell death of B lymphocytes. To test this hypothesis, we purified B cells from the spleens of 6- to 8-week-old healthy transgenic mice and control littermates and stimulated them with LPS or anti-IgM antibody in vitro as described in Materials and Methods. B cells from the transgenic mice were hyperresponsive to mitogenic stimulation by LPS and anti-IgM cross-linking (Fig. 5). In addition, the same transgenic B cells exhibited significant reduction in activation-induced cell death (Fig. 6). After activation with LPS or IgM for 5 days in culture, B cells from transgenic mice exhibited significantly prolonged survival compared with B cells from nontransgenic littermates (Fig. 6A and B, respectively). On the basis of cell size and surface marker staining, surviving cells were large IgG^+ B lymphocytes (data not shown). Furthermore, freshly isolated IgG^+ B cells from 12-week-old transgenic mice also exhibited prolonged survival even in the absence of any exogenous stimuli in vitro (Fig. 6C).

Other pathologies of *Fli-1* transgenic mice. In contrast to the kidney abnormalities, splenomegaly, and lymphoid abnormalities described above, the brains, livers, hearts, lungs, skeletal muscles, gonads, and digestive tracts of the transgenic mice showed no gross histological abnormalities. However, at the late stages of the disease, small numbers of lymphocytes and plasma cells were observed in the livers, lungs, pancreases, and joints of the diseased mice. Furthermore, almost all the mice with late-stage renal disease had severe anemia (data not shown).

DISCUSSION

In this paper, we have described three lines of transgenic mice that express elevated levels of Fli-1, a member of the Ets family of DNA-binding proteins. These mice developed a progressive immunological renal disease, which ultimately led to death and was associated with altered numbers and phenotypes of both B and T cells. Thus, these data suggest that Fli-1, which is normally highly expressed in lymphoid cells, is an important regulator of lymphoid cell function. During the analysis of *Fli-1* gene expression in *H-2K^k–Fli-1* transgenic mice, we observed that endogenous *Fli-1* transcripts increased by two- to threefold in those tissues in which the *Fli-1* transgene was also expressed. This observation raises the possibility that *Fli-1* is upregulated in *trans* as a result of the overexpression of the *Fli-1* transgene, either directly as a result of possible *Fli-1* DNA binding sites in its own transcriptional regulatory region or indirectly through the activation of downstream genes that can activate Fli-1.

The frequency of renal disease correlated with the levels of *Fli-1* expression in the lymphoid tissues of the transgenic mice (B6 > B7 > B8). For example, the B6 line had the highest transgene copy number and the highest Fli-1 protein level in the thymus and spleen and also developed renal disease with the highest incidence at each age group. In contrast, the B8 line, which has the lowest transgene copy number and no increased *Fli-1* transcripts in the thymus and spleen, had an incidence of renal disease in each age group indistinguishable from that of control mice. High levels of *Fli-1* expression were observed only in the infiltrating lymphocytes in diseased kidneys, as shown by RNA in situ analysis. These data suggest that *Fli-1* gene expression in lymphoid tissues significantly correlated with the development of renal disease in *Fli-1* transgenic mice and that the renal disease that developed in these mice was not the direct consequence of *Fli-1* transgene expression in the kidney. It is interesting that the dramatic perturbations in lymphocyte cell populations observed in these mice, and the resulting kidney pathology, were associated with relatively small changes in Fli-1 protein levels. Together, these data argue that lymphoid cells are highly sensitive to perturbations in the level of *Fli-1* expression. As the *Fli-1* transgene was driven by the heterologous *H-2K^k* class I promoter, it is also possible that the *Fli-1* transgene is expressed in cells which

TABLE 4. Comparison of *Fli-1* transgenic mice with other autoimmune mouse models[a]

Mice	Mutation or transgene	Immune-complex glomerulo-nephritis	Lymph-adenopathy	Spleno-megaly	B-cell hyperplasia	Autoreactive lymphocyte	Autoantibodies	Reference
lpr/lpr	FAS−/−	Yes	Yes	Yes	Yes	$CD3^+$ $B220^+$	Anti-DNA	7
NZB/NZW	Unknown	Yes	No	Yes	Yes	$CD5^+$ $B220^+$	Antierythrocyte, antithymocyte	24
Bcl-2 transgenic	*Eμ–Bcl-2*	Yes	No	Yes	Yes (prolonged survival)	No	Antinucleus	28
Fli-1 transgenic	*H-2K^k–Fli-1*	Yes	No	Yes	Yes	$CD3^+$ $B220^+$, $CD5^+$ $B220^+$ (only late stage)	Antinucleus, anti-DNA	

[a] The immunologic phenotypic characteristics of *Fli-1* transgenic mice compared with those of other murine models of autoimmune disease.

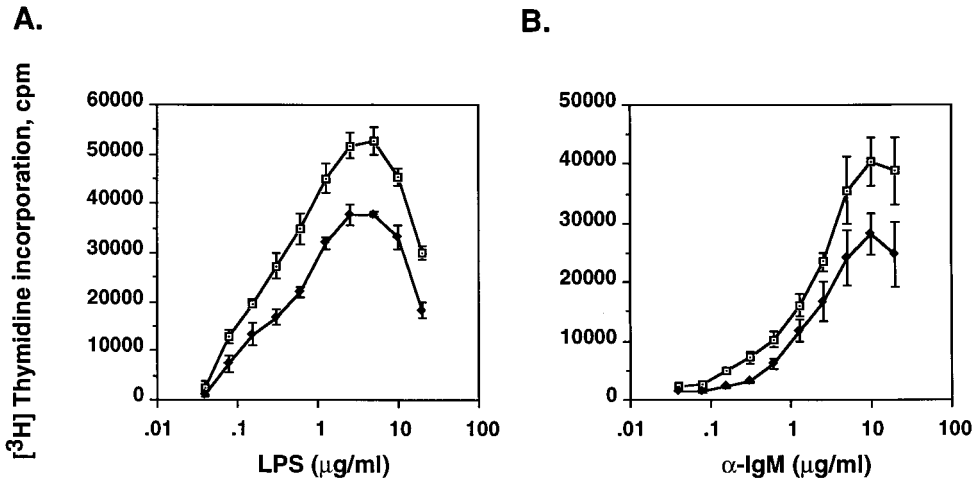

FIG. 5. Mitogenic stimulation of B cells from *Fli-1* transgenic and control mice. B cells from *Fli-1* transgenic (⊡) and control mice (◆) were cultured in LPS (Sigma) for 3 days (A) or anti-IgM (α-IgM) (Sigma) for 2 days. (B) Proliferative responses were determined by measuring [^{3}H]thymidine incorporation at different concentrations of LPS or anti-IgM. The data shown here are from one of four representative experiments. B-cell proliferation is significantly increased for *Fli-1* transgenic mice for LPS ($P < 0.02$ by Student's t test) and anti-IgM ($P < 0.012$ by Student's t test).

normally do not express Fli-1 and that ectopic *Fli-1* expression could affect the expression of genes that contain DNA binding sites for Fli-1 in their transcriptional regulatory regions.

Histologically, the early stage of renal disease was characterized by tubulointerstitial nephritis but only minor changes in the glomeruli. The massive interstitial infiltration of lymphocytes occurred in the absence of immunoglobulin deposition along the tubular basement membranes. In many areas, the renal tubules were dilated and/or filled with immunoglobulin casts, suggesting that a degree of obstruction may also have contributed to the tubulointerstitial disease. In contrast to the tubulointerstitial nephritis, glomerular injury occurred later and was closely associated with the appearance of immune complexes, particularly along the subendothelial areas of the glomerular capillary wall and within the mesangium. On the basis of the presence of polyclonal immunoglobulin and C3 and by their homogenous electron-dense appearance by electron microscopy, we assume that the intraglomerular deposits represent immune complexes, although the nature of the target antigen is unknown. Lack of staining with Congo red makes it unlikely that these deposits are amyloid proteins, and the absence of a fibrillar pattern to the deposits also makes it unlikely that the depositions are amyloid proteins or cryoglobulins.

The *Fli-1* transgenic mice also developed B-cell hyperplasia, splenomegaly, and hypergammaglobulinemia, which was closely associated with the progression of immune-complex renal disease. The animals developed hypergammaglobulinemia prior to the onset of proteinuria, suggesting that polyclonal B-cell activation occurred first, although the antigens that caused such a cellular immune response are not known. No monoclonal immunoglobulin peaks were observed by immunoelectrophoresis, excluding the possibility of a B-cell malignancy. In vitro studies demonstrated that B cells from *Fli-1* transgenic mice were hyperresponsive to mitogenic stimuli. In addition, B cells from the *Fli-1* transgenic mice were relatively refractory to mitogen-induced activation of cell death in vitro (4). The IgG^+ B cells and plasma cells that exhibited prolonged survival in vitro also accumulated in late-stage diseased kidneys in vivo, suggesting that these infiltrating B cells were

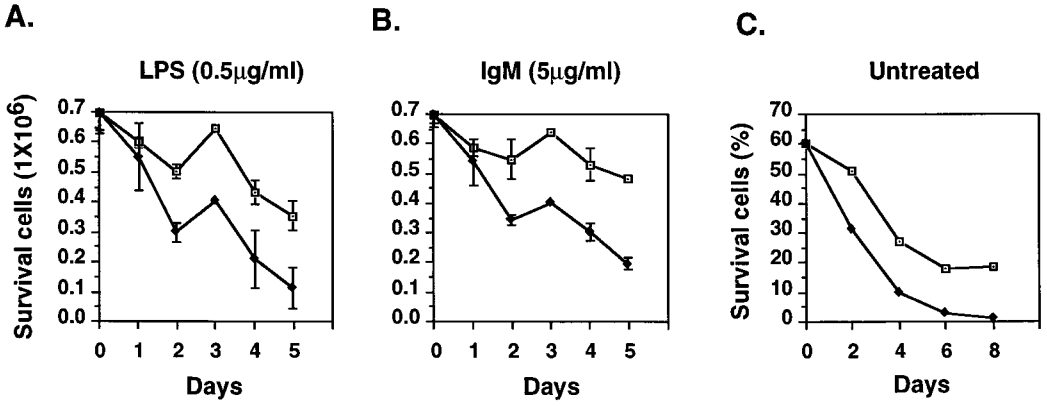

FIG. 6. Survival of B cells from *Fli-1* transgenic mice and control littermates. (A and B) Survival of purified B cells from healthy transgenic mice (⊡) and control littermates (◆) measured by trypan blue exclusion after treatment with LPS (0.5 μg/ml) or anti-IgM (5 μg/ml) for different incubation times. Means and standard errors are shown. (C) Survival of B cells from 12-week-old transgenic mice (⊡) and control littermates (◆) measured by flow cytometry with propidium iodide for hypodiploid nuclei at the indicated times. Percentages indicate viable cells among total cells in the culture. The data shown are from one of three representative experiments.

involved in the development of immunological renal disease. This possibility is consistent with other murine models of autoimmune renal disease that also display B-cell hyperplasia (Table 4). Interestingly, transgenic mice that overexpress *Bcl-2*, an antiapoptosis gene (26, 32), in B cells exhibit an enhanced antibody response and prolonged survival in vitro and develop a systemic autoimmune disease in vivo (28). As the *Fli-1* transgenic mice exhibited a B-cell dysfunction similar to that of *Eμ–Bcl-2* transgenic mice, it is possible that *Fli-1* overexpression interferes with programmed cell death in B cells, resulting in a similar autoimmune renal disease. However, this effect on B cells may be a direct consequence of *Fli-1* transgene expression or may be an indirect consequence of transgene expression in another cell type, particularly T cells. In contrast to these striking changes in B-cell populations, there were no significant differences in the distribution of $CD4^+$ and $CD8^+$ thymocytes in the transgenic mice compared with that of control littermates (data not shown). In addition, there was also no significant difference in the survival of thymocytes placed in culture over a 5-day period (data not shown).

Several lines of evidence suggest that an autoimmune mechanism underlies the renal disease observed in *Fli-1* transgenic mice: (i) the polyclonal B-cell activation and hypergammaglobulinemia; (ii) deposition of polyclonal immunoglobulin, immune complexes, and complement C3 in the glomeruli; (iii) accumulation of abnormal T cells ($CD3^+$ $B220^+$) and B cells ($CD5^+$ $B220^+$) in peripheral lymphoid tissues; (iv) formation of antinucleus and anti-double-stranded DNA autoantibodies; (v) prolonged survival of autoreactive B cells to stimuli; and (vi) progressive infiltration of lymphocytes in kidneys. Under normal circumstances, autoantibody secretion is only transient (18). In autoimmune murine models such as *lpr*/*lpr* and NZB/NZW mice, various autoantibodies that react with nucleic acids, nucleoproteins, cell surface antigens, and phospholipids accumulate, causing tissue-specific and nonspecific damage (24). In addition, polyclonal B-cell activation has been considered a crucial component in autoimmunity, particularly in systemic disease (30, 31). The proposition that polyclonal B-cell activators can induce autoantibodies is predicted by the existence of nondeleted self-reactive B cells that might become active upon appropriate stimulation (30). Thus, the accumulation of abnormal $CD5^+$ $B220^+$ B cells, IgG^+ B cells, and plasma cells and the production of autoantibodies in the *Fli-1* transgenic mice are most likely the consequence of polyclonal B-cell activation that developed in the early stage of disease. Therefore, we suggest that the *Fli-1* transgene induces alterations in T- and B-cell function, resulting in polyclonal B-cell activation, prolonged survival of blast IgG^+ B cells, accumulation of autoreactive T and B lymphocytes in the periphery, and eventually, the accumulation of pathogenic levels of anti-self antibodies. It should be noted that we have also occasionally (15%) observed foci of interstitial lymphocyte infiltration in the kidneys of old control mice and one 18-month-old control mouse with immune-complex glomerulonephritis, suggesting that the CD-1 mouse strain used in these experiments may be somewhat predisposed to autoimmune disease. Taken together, our data suggest that overexpression of the *Fli-1* transgene contributes to the development of an autoimmune renal disease.

The *Fli-1* transgenic mice also developed anemia in the late stage of the disease. The hormone erythropoietin, a major positive regulator of erythropoiesis, is synthesized in the kidney. Thus, this anemia is most likely a secondary consequence of renal failure, caused by the severe autoimmune destruction of the kidney.

The immunopathogenic mechanisms that cause progressive renal disease (tubulointerstitial nephritis and glomerulonephritis) in *Fli-1* transgenic mice appear to involve both cellular and humoral immune cascades. The development of immunological renal disease in these mice suggests that Fli-1 may play a critical role in the regulation of both T and B lymphoid cell function. This conclusion is consistent with the expression patterns of Fli-1 in adult mice and the presence of DNA binding sites for Fli-1 in the transcriptional regulatory regions of a number of lymphoid cell-specific genes (13, 19). In addition, the immunological renal disease that develops in *Fli-1* transgenic mice shares a number of features with other mouse models of autoimmunity (31). Table 4 summarizes some of the common and distinct features of the autoimmune disease in *Fli-1* transgenic mice and other murine models. For example, *Fli-1* transgenic mice display elevated levels of both abnormal $CD3^+$ $B220^+$ T cells and $CD5^+$ $B220^+$ B cells. In contrast, *lpr*/*lpr* mice exhibit only increased numbers of $CD3^+$ $B220^+$ T cells, whereas NZB/NZW mice exhibit only increased numbers of $CD5^+$ $B220^+$ B cells (Table 4). On the other hand, the autoimmune immune-complex glomerulonephritis that develops in *Eμ–Bcl-2* transgenic mice is not associated with the accumulation of abnormal $CD3^+$ $B220^+$ T or $CD5^+$ $B220^+$ B lymphocytes (28). Thus, *Fli-1* transgenic mice provide a unique animal model to study the molecular and cellular bases of immunological renal disease. *Fli-1* transgenic mice also display immunopathologic and serologic features that closely resemble human systemic lupus erythematosus, making these mice a potentially useful model to study this disease. Finally, *Fli-1* transgenic mice should be useful in identifying target genes regulated by *Fli-1* in vivo, particularly those genes that control activation and programmed cell death of lymphocytes.

ACKNOWLEDGMENTS

We thank Dragana Cado and Wilson Khoo for generation of the *Fli-1* transgenic mice; Sandra Gardner and Jessie Luna for maintenance of the animals; Dorothy Wilkins for help in biochemical analysis; and Yvan Bedard, Douglas Holmyard, Jackie Pittman, and Helena Sustackova for preparation of electron micrographs and histological sections. We are grateful to Ken Harpal for help with histology. We thank Josef Penninger, Atsuo Ochi, Jonathan Lee, C. C. Hui, and Alec Chen for thoughtful discussions during the preparation of the manuscript. We thank John Abrahamson, Bob Paulson, Jacques Bollekens, and other members of the Bernstein laboratory for help and comments throughout this work.

This work was supported by a Terry Fox Program Project Grant from the National Cancer Institute of Canada. A.B. is an International Scholar of the Howard Hughes Medical Institute.

REFERENCES

1. **Adams, J. M., A. W. Harris, C. A. Pinkert, C. M. Corcorant, W. S. Alexander, S. Cory, R. D. Palmiter, and R. L. Brinster.** 1985. The c-myc oncogene driven by immunoglobulin enhancers induces lymphoid malignancy in transgenic mice. Nature (London) **318:**533–538.
2. **Ben-David, Y., E. B. Giddens, and A. Bernstein.** 1990. Identification and mapping of a common proviral integration site *Fli-1* in erythroleukemia cells by Friend murine leukemia virus. Proc. Natl. Acad. Sci. USA **87:**1332–1336.
3. **Ben-David, Y., E. B. Giddens, K. Letwin, and A. Bernstein.** 1991. Erythroleukemia induction by Friend murine leukemia virus: insertional activation of a new member of the ets gene family, Fli-1, closely linked to c-ets-1. Genes Dev. **5:**908–919.
4. **Chaouchi, N., A. Vazquez, P. Galanaud, and C. Leprince.** 1995. B cell antigen receptor-mediated apoptosis: importance of accessory molecules CD19 and CD22, and of surface IgM cross-linking. J. Immunol. **154:**3096–3104.
5. **Chomczynski, P., and N. Sacchi.** 1987. Single-step method of RNA isolation by acid guanidinium thiocyanate-phenol-chloroform extraction. Anal. Biochem. **162:**156–159.
6. **Daar, A. S., S. V. Fuggle, J. W. Fabre, A. Ting, and P. J. Morris.** 1984. The detailed distribution of HLA-A, B, C antigens in normal human organs. Transplantation **38:**287–291.
7. **Davidson, W. F., F. J. Dumont, H. G. Bedigian, B. J. Fowlkes, and H. C.**

Morse III. 1986. Phenotypic, functional, and molecular genetic comparisons of the abnormal lymphoid cells of C3H-*lpr*/*lpr* and C3H-*gld*/*gld* mice. J. Immunol. **136:**4075–4084.
8. **Delattre, O., J. Zucman, B. Plougastel, C. Desmaze, T. Melot, M. Peter, H. Kovar, I. Joubert, P. Jong, G. Rouleau, A. Aurias, and G. Thomas.** 1992. Gene fusion with an ETS DNA-binding domain caused by chromosome translocation in human tumours. Nature (London) **359:**162–165.
9. **Ellis, C., E. Clauser, D. O. Morgan, M. Edery, R. A. Roth, and W. J. Rutter.** 1986. Replacement of insulin receptor tyrosine residues 1162 and 1163 compromises insulin stimulated kinase activity and uptake of 2-deoxyglucose. Cell **45:**721–732.
10. **Foster, M. H., B. Cizman, and M. P. Madaio.** 1993. Biology of disease: nephritogenic autoantibodies in systemic lupus erythematosus: immunochemical properties, mechanisms of immune deposition, and genetic origins. Lab. Invest. **69:**494–507.
11. **Fritzler, M. J., and E. M. Tan.** 1985. Antinuclear antibodies and the connective tissue disease, p. 207–247. *In* A. S. Cohen (ed.), Laboratory diagnostic procedures in the rheumatic diseases. Grune and Stratton, New York.
12. **Golub, T. R., G. F. Barker, M. Lovett, and D. G. Gilliland.** 1994. Fusion of PDGF receptor beta to a novel *ets*-like gene, *tel*, in chronic myelomonocytic leukemia with t(5;12) chromosomal translocation. Cell **77:**307–316.
13. **Hagman, J., and R. Grosschedl.** 1994. Regulation of gene expression at early stages of B-cell differentiation. Curr. Opin. Immunol. **6:**222–230.

13a. **Hathcock, K. S.** 1992. T cell depletion by cytotoxic elimination, p. 3.4.1–3.4.8. *In* J. E. Coligan, A. M. Kruisbeek, D. H. Margulies, E. M. Shevach, and W. Strober (ed.), Current protocols in immunology, vol. 1. John Wiley & Sons, Inc., New York.

14. **Hayakawa, K., and R. R. Hardy.** 1988. Normal, autoimmune and malignant $CD5^+$ B cells: the Ly-1 B lineage? Annu. Rev. Immunol. **6:**197–218.
15. **Hayakawa, K., R. R. Hardy, M. Honda, L. A. Herzenberg, A. D. Steinberg, and L. A. Herzenberg.** 1984. Ly-1 B cells: functionally distinct lymphocytes that secrete IgM autoantibodies. Proc. Natl. Acad. Sci. USA **81:**2494–2498.
16. **Kimura, A., A. Israel, L. B. Odile, and P. Kourilsky.** 1985. Detailed analysis of the mouse H-$2K^b$ promoter: enhancer-like sequences and their role in the regulation of class I gene expression. Cell **44:**261–272.
17. **Klemsz, M. J., R. A. Maki, T. Papayannopoulou, J. Moore, and R. Hromas.** 1993. Characterization of the ets oncogene family member, fli-1. J. Biol. Chem. **268:**5769–5773.
18. **Klinman, D. M., and A. D. Steinberg.** 1987. Systemic autoimmune disease arises from polyclonal B cell activation. J. Exp. Med. **165:**1755–1760.
19. **Leiden, J. M., and C. B. Thompson.** 1994. Transcriptional regulation of T cell genes during T-cell development. Curr. Opin. Immunol. **6:**231–237.
20. **Macleod, K., D. Leprince, and D. Stehelin.** 1992. The ets gene family. Trends Biochem. Sci. **17:**251–256.
21. **May, W. A., M. L. Gishizky, S. L. Lessnick, L. B. Cunsford, B. C. Lewis, O. Delattre, J. Zucman, G. Thomas, and C. T. Denny.** 1993. The Ewing's sarcoma EWS/Fli-1 fusion gene encodes a more powerful transforming gene than Fli-1. Proc. Natl. Acad. Sci. USA **90:**5752–5756.
22. **McCracken, S., S. Leung, R. Bosselut, J. Ghysdael, and N. G. Miyamoto.** 1994. Myb and Ets related transcription factors are required for activity of the human *lck* type I promoter. Oncogene **9:**3609–3615.
23. **Motro, B., D. Van Der Kooy, J. Rossant, A. Reith, and A. Bernstein.** 1991. Contiguous patterns of *c-kit* and *Steel* expression: analysis of mutations at the W and Sl loci. Development **113:**1207–1221.
24. **Pankewycz, O. G., P. Migliorini, and M. P. Madaio.** 1987. Polyreactive autoantibodies are nephritogenic in murine lupus nephritis. J. Immunol. **139:**3287–3294.
25. **Rivera, R. R., M. H. Stuiver, R. Steenbergen, and C. Murre.** 1993. Ets proteins: new factors that regulate immunoglobulin heavy-chain gene expression. Mol. Cell. Biol. **13:**7163–7169.
26. **Sentman, C. L., J. R. Shutter, D. Hockenbery, O. Kanagawa, and S. J. Korsmeyer.** 1991. Bcl-2 inhibits multiple forms of apoptosis but not negative selection in thymocytes. Cell **67:**879–888.
27. **Seth, A., R. Ascione, R. J. Fisher, G. J. Mavrothalassitis, N. K. Bhat, and T. S. Papas.** 1992. The ets gene family. Cell Growth Differ. **3:**327–334.
28. **Strasser, A., S. Whittingham, D. L. Vaux, M. L. Bath, J. M. Adams, S. Cory, and A. W. Harris.** 1991. Enforced BCL2 expression in B-lymphoid cells prolongs antibody responses and elicits autoimmune disease. Proc. Natl. Acad. Sci. USA **88:**8661–8665.
29. **Tan, E. M.** 1989. Antinuclear antibodies: diagnostic markers for autoimmune diseases and probes for cell biology. Adv. Immunol. **44:**93.
30. **Theofilopoulos, A. N.** 1993. T-cell receptor genes in autoimmunity. Ann. N. Y. Acad. Sci. **681:**33–46.
31. **Theofilopoulos, A. N.** 1995. The basis of autoimmunity. Part I. Mechanisms of aberrant self-recognition. Immunol. Today **16:**90–98.
32. **Veis, D. J., C. M. Sorenson, J. R. Shutter, and S. J. Korsmeyer.** 1993. Expression of the Bcl-2 protein in murine and human thymocytes and in peripheral T lymphocytes. Cell **75:**229–240.
33. **Zhang, L., V. Lemarchandel, P. H. Romeo, Y. Ben-David, P. Greer, and A. Bernstein.** 1993. The *Fli-1* proto-oncogene, involved in erythroleukemia and Ewing's sarcoma, encodes a transcriptional activator with DNA-binding specificities distinct from other Ets family members. Oncogene **8:**1621–1630.
34. **Zhou, T., H. Bluethmann, J. Eldridge, K. Berry, and J. D. Mountz.** 1993. Origin of $CD4^-CD8^-B220^+$ T cells in MRL-*lpr*/*lpr* mice. J. Immunol. **150:**3651–3667.
35. **Zucman, J., T. Melot, C. Desmaze, J. Ghysdael, B. Plougastel, M. Peter, J. M. Zuchker, T. J. Triche, K. Sheer, C. Turc-Carel, P. Ambros, V. Combaret, G. Lenoir, A. Auras, G. Thomas, and O. Delattre.** 1993. Combinatorial generation of variable fusion proteins in the Ewing family of tumours. EMBO J. **12:**4481–4487.